MEMBRANE DIFFERENTIATIONS AT SITES SPECIALIZED FOR CELL FUSION

RICHARD L. WEISS, DANIEL A. GOODENOUGH, and URSULA W. GOODENOUGH

From the Biological Laboratories, Harvard University, Cambridge, Massachusetts 02138, and the Department of Anatomy, Harvard University Medical School, Boston, Massachusetts 02115. Dr. Weiss's present address is the Department of Medical Microbiology, University of California, Irvine, California 92664.

ABSTRACT

Fusion of plasma membranes between *Chlamydomonas reinhardtii* gametes has been studied by freeze-fracture electron microscopy of unfixed cells. The putative site of cell fusion develops during gametic differentiation and is recognized in thin sections of unmated gametes as a plaque of dense material subjacent to a sector of the anterior plasma membrane (Goodenough, U. W., and R. L. Weiss. 1975. *J. Cell Biol.* **67**:623–637). The overlying membrane proves to be readily recognized in replicas of unmated gametes as a circular region roughly 500 nm in diameter which is relatively free of "regular" plasma membrane particles on both the P and E fracture faces. The morphology of this region is different for mating-type plus (mt^+) and mt^- gametes: the few particles present in the center of the mt^+ region are distributed asymmetrically and restricted to the P face, while the few particles present in the center of the mt^- region are distributed symmetrically in the E face. Each gamete type can be activated for cell fusion by presenting to it isolated flagella of opposite *mt*. The activated mt^+ gamete generates large expanses of particle-cleared membrane as it forms a long fertilization tubule from the mating structure region. In the activated mt^- gamete, the E face of the mating structure region is transformed into a central dome of densely clustered particles surrounded by a particle-cleared zone. When mt^+ and mt^- gametes are mixed together, flagellar agglutination triggers similar activation events, but the tip of each mt^+ fertilization tubule proceeds to fuse with an activated mt^- region. The fusion lip is seen to develop within the particle-dense central dome. We conclude that these mt^- particles play an active role in membrane fusion.

Cell fusion initiates the sexual process in both lower and higher eukaryotes, but the mechanism(s) by which the participating membranes actually fuse with one another remains largely unknown. Experiments with model membrane systems have established that lipid bilayers are inherently very stable structures (28) which must be "conditioned" by some destabilizing agent or process if they are to fuse with one another (reviewed in reference 29). While a number of such "fusogenic agents" have been identified in vitro–including certain fatty acids or lipids (1, 2, 25, 27), detergents (8, 26, 40), and ionic or thermal conditions (4, 8, 19, 37–39, 50); it is not known which,

if any, of these agents or conditions operates during natural cell fusion.

We present here a freeze-fracture study of gametic cells of the biflagellate *Chlamydomonas reinhardtii* whose plasma membranes become specialized for fusion during gametic differentiation. This fusion process has several advantages as an experimental system. First, it occurs between "naked" cell membranes and proceeds with 100% efficiency (18, 30). Second, it is not necessary to introduce a virus or an external agent (e.g., an ionophore) to achieve cell fusion and the interpretation of freeze-fracture replicas is therefore not confused by nonfusion-related perturbations of the cell caused by such agents (cited, for example, in references 36 and 37). Third, cell fusion is restricted to a localized site at the anterior of each gamete; these sites have been well characterized by transmission electron microscopy (10, 16, 18, 48) and prove to be easily recognizable in freeze-fracture replicas. Finally, the gametes are of two mating types (mt^+ and mt^-), and each type develops fusion competency in the absence of the other; therefore, membrane differentiations that anticipate cell fusion can be distinguished from membrane changes that accompany cell fusion.

MATERIALS AND METHODS

Chlamydomonas reinhardtii strain 137c-H (17), mt^+ and mt^-, served as wild type. The mutant *imp-1* mt^+ strain was used in certain experiments, and it proved to have altered its properties since the time it was originally described (17, 18): a small proportion of the cells are now capable of generating an abnormally short, broad fertilization tubule in which the microfilaments do not remain extended. Further information on this leaky condition will be published elsewhere.

Gametes were prepared from week-old plate cultures as previously described (30). Cells were prepared for freeze-cleave and freeze-etch electron microscopy as described by Bergman et al. (6). No fixatives or cryoprotective agents were used at any point (see reference 31).

Isolated flagella were prepared as follows. Gametes of one mating type were suspended in 5 ml of nitrogen-free high-salt minimal medium (NF-HSM) (30) to which 25 μl of 1.25 μg/μl amphotericin dissolved in dimethylsulfoxide (DMSO) were added. Within 5 min, flagella were quantitatively detached from the cells and curled up into membrane-limited disks. Cells were pelleted at 3,000 *g* and the flagellar disks were pelleted at 31,000 *g*; these were suspended in a small volume of NF-HSM. To activate mating structures for freeze-cleave electron microscopy, gametes of one mating type were mixed with the flagellar disks of opposite mating type at a ratio of 1:5 and allowed to agglutinate for 15 min. The cells were then pelleted by a rapid centrifugation at 3,000 *g* and applied in small concentrated drops to paper disks for freezing.

The cell shown in Fig. 1 was incubated in 10% DMSO in NF-HSM for 10 min at room temperature, pelleted, and then fixed in 4% glutaraldehyde in 10 mM potassium phosphate buffer, pH 7, with 1 mM $CaCl_2$ for 5 min, postfixed in a glutaraldehyde-OsO_4 mixture for 1 h (30), dehydrated, and embedded. The cell shown in Fig. 2 was chilled, fixed in cold 0.0008% glutaraldehyde in HEPES buffer (18) for 15 min, after which it was treated with cold 0.5% OsO_4 for 1 h, dehydrated, and embedded. Both protocols result in an extensive extraction of cytoplasm which allows a particularly clear view of mating structure organization in thin section.

RESULTS

General Features of Gametic Differentiation

A detailed study of the events resulting in cell fusion between *C. reinhardtii* gametes has been recently presented from our laboratory (18) and we summarize here only those features that are essential to the interpretation of the freeze-fracture replicas presented in subsequent sections.

Gametes of *C. reinhardtii* differentiate in response to nitrogen starvation but not in response to any physical or chemical signal from the other mating type. As a result, vegetative mt^+ and mt^- *C. reinhardtii* cells (which lack the capacity to undergo cell fusion) can be cultured separately and starved of nitrogen, resulting in cultures of unmated mt^+ gametes and unmated mt^- gametes. When an unmated mt^+ or mt^- gamete is examined in thin section, each proves to possess a mating structure, a dense curved region associated with its anterior cell membrane and acquired during gametic differentiation (30). Particularly detailed images of these structures can be obtained by using the fixation procedures described in Materials and Methods. In the unmated mt^+ mating structure (Fig. 1), a continuous narrow membrane zone adheres to the inner leaflet of the plasma membrane and a broader doublet zone lies beneath it; this doublet zone has the three-dimensional shape of an asymmetric or "lopsided" collar (16). Evident also are fine extensions from the outer membrane surface (Fig. 1, arrow) which may represent carbohydrate. The mating structure of an unmated mt^- gamete (Fig. 2) possesses a broad membrane zone and lacks a doublet zone, although by the present fixation method a distinct layer of material can be recognized beneath the membrane

zone at the periphery of the mating structure (Fig. 2, arrows). Both types of mating structure are found to one side of the basal-body complex at the cell anterior, and are intimately associated with bands of microtubules that extend from the basal body region (Weiss and Goodenough, manuscript in preparation).

Mating is initiated when mt^+ and mt^- gametes are mixed, and normally commences with an agglutination between mt^+ and mt^- flagellar tips (reviewed in reference 6). Agglutination triggers mating structure activation. In mt^+ cells the mating structure everts to form a small bud, the membrane zone becomes discontinuous medially and the bud protrudes further, and finally, the doublet zone appears to attach to the membrane and puts out an array of microfilaments which rapidly extend into the bud to form a long, narrow fertilization tubule (10, 16, 18, 48). The mating structures of mt^- cells undergo no such dramatic changes during early activation, but the membrane zone often appears medially discontinuous and may open up completely during a prolonged activation (18).

Cell fusion is initiated when the tip of the fertilization tubule meets the activated mt^- structure, resulting in the formation of a narrow cytoplasmic bridge filled with microfilaments. The bridge appears to shorten and widen and then opens to allow lateral confluence between the gametes and the formation of a quadriflagellate zygotic cell.

Membrane Associated with the Unactivated mt^+ Mating Structure

As detailed in the previous paper (52), the anterior plasma membrane of *C. reinhardtii* reveals a number of internal differentiations when examined by freeze-fracture electron microscopy. Both vegetative and gametic membranes exhibit the flagellar bracelets, strut arrays, and contractile vacuole aggregates described in the previous paper, but gametes possess an additional membrane differentiation which invariably lies adjacent to one of the two flagellar bracelets and nearer to the bracelets than the contractile vacuole. Since this is precisely the expected location of the mating structure (16, 18) and since it is absent from vegetative cells, this differentiated region is readily identified as being related to the gametic mating structure.

Figs. 3–5 show representative freeze-fracture replicas of this region in unmated mt^+ gametes as viewed in the P (protoplasmic) half of the membrane. The region, which is round or ellipsoid, is seen in Fig. 3 to lie between a flagellar bracelet and a contractile-vacuole crater and to carry a reduced number of particles compared to the surrounding plasma membrane. Particles are typically absent from the periphery of the region. The particles present in the interior of the region may be quite sparse (Figs. 4 and 5) or more abundant (Fig. 3); in either case, the particulate sector (la-

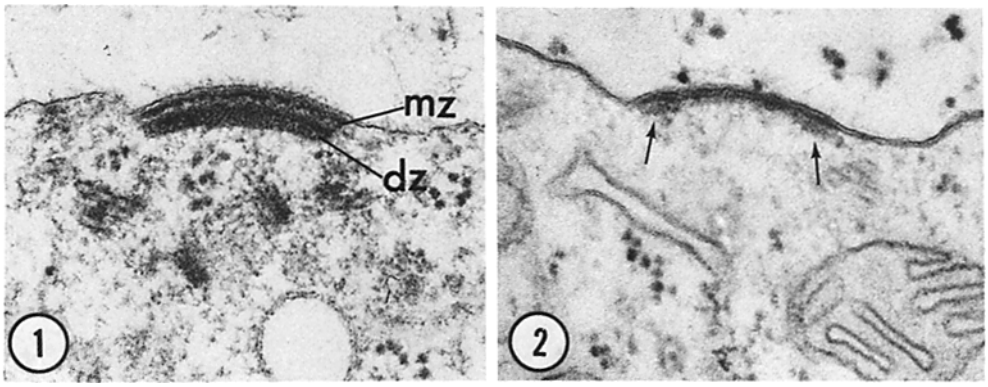

FIGURE 1 Mating structure of an mt^+ gamete showing the narrow membrane zone (*mz*) underlying the plasma membrane and the broad doublet zone (*dz*) beneath. Fine hairlike projections extend outward from the plasma membrane overlying the mating structure. A young basal body and several microtubules are present in the underlying cytoplasm. × 86,000.

FIGURE 2 Mating structure of an mt^- gamete showing the membrane zone beneath the plasma membrane which thickens somewhat at both edges of the structure (arrows). × 86,000.

beled *p* in Figs. 3 and 4) localizes to one side of center, an asymmetry which contrasts to the symmetrical disposition of particles in a contractile vacuole aggregate (52). The nonparticulate sector of the central mt^+ region may exhibit a finely granular substructure (e.g., Fig. 4) and a string of particles identical to a bracelet strand may mark one edge of the structure (e.g., Fig. 5, arrow).

A 1-min etching of the fractured P membrane face dramatizes the differentiation of the mt^+ mating structure region (Fig. 6). Whereas the etching processes tend to "explode" the surrounding particle-containing membrane, the mating structure is apparently undisturbed and stands out in obvious relief. The bracelet and necklace arrays, it should be noted, are also unaffected by etching, whereas the contractile vacuole region is rendered unrecognizable.

The complementary E (ectoplasmic) face of the unmated mt^+ structure is shown in Fig. 7. A striking exclusion of plasma membrane particles is evident in this face as well; the few particles present tend to localize asymmetrically to one side of the central region. Evident also in Fig. 7 and in other mt^+ E-face replicas is a textural difference in the background, the lower half of the structure appearing roughened relative to the upper half. Since such differences can be caused by changes in shadowing angle and since the structure is curved, we are unable to determine whether this asymmetry is induced by the technique and/or reflects an underlying structural asymmetry in the E face which might correspond to the asymmetry noted in the P face.

Membrane Associated with the Unactivated mt^- Mating Structure

The membrane differentiation associated with the mt^- mating structure tends to be somewhat smaller than the mt^+ region; whereas the mt^+ region has an average diameter of 530 nm, the mt^- region averages 340 nm. A similar size difference is evident in thin sections, where a typical mt^+ structure occupies eight serial sections and an mt^- structure five serial sections. We should note, however, that these are average values and that mt^+ structures, in particular, vary considerably in size.

Figs. 8 and 9 show two mt^- structures as seen in a freeze-fractured P face. The images are typical except for the ridge of material that arcs around one edge of the structure in Fig. 8; such configurations, while rather common for mt^+ mating structures (e.g., Fig. 5), are rare for mt^-. The mt^- mating structure is similar to its mt^+ counterpart in that it excludes most plasma membrane particles. It is distinctive, however, in two respects. (*a*) It lacks the few large particles that are found in the *p* sector of the mt^+ P face (Figs. 3 and 4). (*b*) It possesses a cluster of small particulate material that is symmetrically distributed within the center of the region, in contrast to the asymmetric placement of the *p* sector of the mt^+ structure (Fig. 4). The mt^- mating structure is, moreover, readily distinguished from a contractile vacuole array by the very small size of its particulate materials (compare with Figs. 8–11 of the reference 52) as well as by its position close to the flagellar bracelet.

That the central region of the mt^- structure is fundamentally different from its mt^+ counterpart is revealed by etching: the center of the mt^- structure "explodes" during a 1-min etching (Fig. 10), in marked contrast to the "unetchable" center of the mt^+ structure (Fig. 6). We should note in passing that the true outer surface of the mt^- mating structure, as revealed by etching in one fortuitous replica, exhibits no obvious substructure.

The E face of the unactivated mt^- mating structure is also different from its mt^+ counterpart. As seen in Fig. 11, the center of the region carries a relatively abundant population of particles (compare with Fig. 7), and no asymmetric particle distribution is encountered. An etched image of the E face has not been obtained for either mating type, possibly because etching destroys the membrane landmarks that we utilize to identify this face (52).

Procedures for Mating Structure Activation

When wild-type mt^+ and mt^- gametes are mixed together at room temperature, virtually all the cells in the mixture complete cell fusion during the 5–10 min required to pellet the cells and prepare the grids, and the resultant replicas are filled with quadriflagellated zygotes of the type shown in Fig. 12. Since all traces of the fusion process are erased in such cells, methods were developed to visualize mating structure activation in the absence of cell fusion so that any "fusion preparation" alterations in the membrane could be observed independently of the fusion process itself.

Images of mt^+ mating-structure activation were obtained in three ways: (*a*) mt^+ gametes were

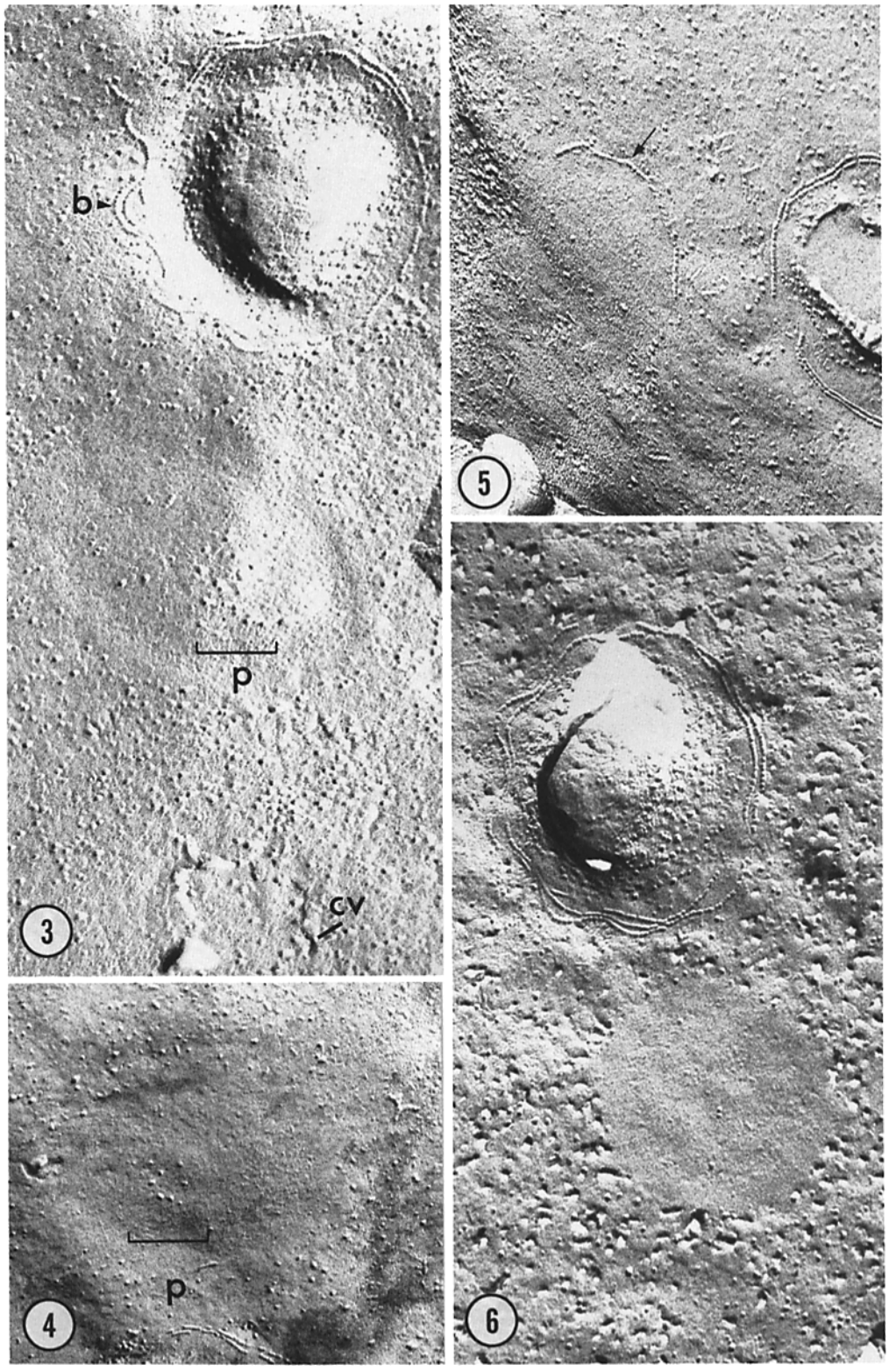
b
p
cv
3
4
5
6

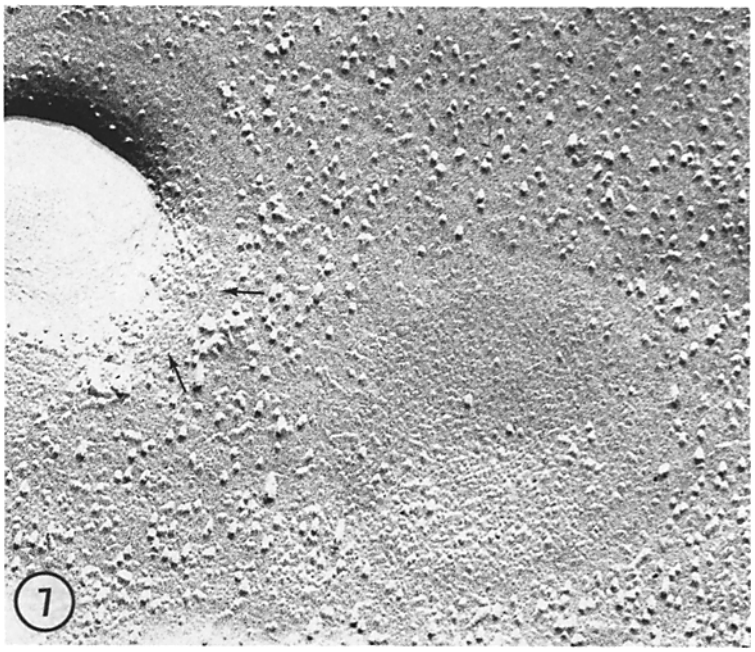

FIGURE 7 Unmated mt^+ gamete (freeze-fracture, E face). Bracelet grooves (arrows) (reference 52) surround the flagellum. The circular mating structure at the lower right is essentially particle-free (see text). × 86,000.

mixed with isolated mt^- gametic flagella; (*b*) a leaky clone of the *imp-1* strain, which occasionally generates a short fertilization tubule but fuses with very low efficiency, was mixed with mt^- gametes; and (*c*) mt^+ and mt^- gametes were separately chilled to 4°C and then mixed together at 4°C for 15–30 min. All three procedures stimulate flagellar agglutination, cell wall lysis, and fertilization tubule extension but allow little or no cell fusion, and all prove to yield comparable freeze-fracture replicas.

Images of mt^- mating-structure activation were produced by two similar methods, again with comparable results: (*a*) mt^- gametes were presented with mt^+ flagella; and (*b*) mt^- gametes were mixed with *imp-1* gametes. The third approach, that of mixing chilled cells at 4°C, yielded no images of activated mt^- mating structures, suggesting that a cold sensitivity of mt^- activation may explain the cold sensitivity of cell fusion. We are currently exploring this possibility. The mode of mating-structure activation employed for each of the following figures is indicated in the various figure legends.

Membrane Changes in Activated mt^+ Mating Structures

Figs. 13–16 show what we interpret to be successive stages in the mt^+ activation process, as viewed

FIGURE 3 Unmated mt^+ gamete (freeze-fracture, P face). Mating structure lies between a flagellar bracelet (*b*) and a contractile vacuole crater (*cv*) (see reference 52). The few particles present in the mating structure cluster to one side of its central portion (*p*). × 86,000.

FIGURE 4 Unmated mt^+ gamete (freeze-fracture, P face). Mating structure possesses a particulate (*p*) sector. × 86,000.

FIGURE 5 Unmated mt^+ gamete (freeze-fracture, P face). A string of particles (arrow) defines one edge of the mating structure region; its relationship, if any, to a bracelet strand (52) is not known. × 86,000.

FIGURE 6 Unmated mt^+ gamete (freeze-etch, P face). The circular mating structure has resisted the etching of the surrounding plasma membrane. × 86,000.

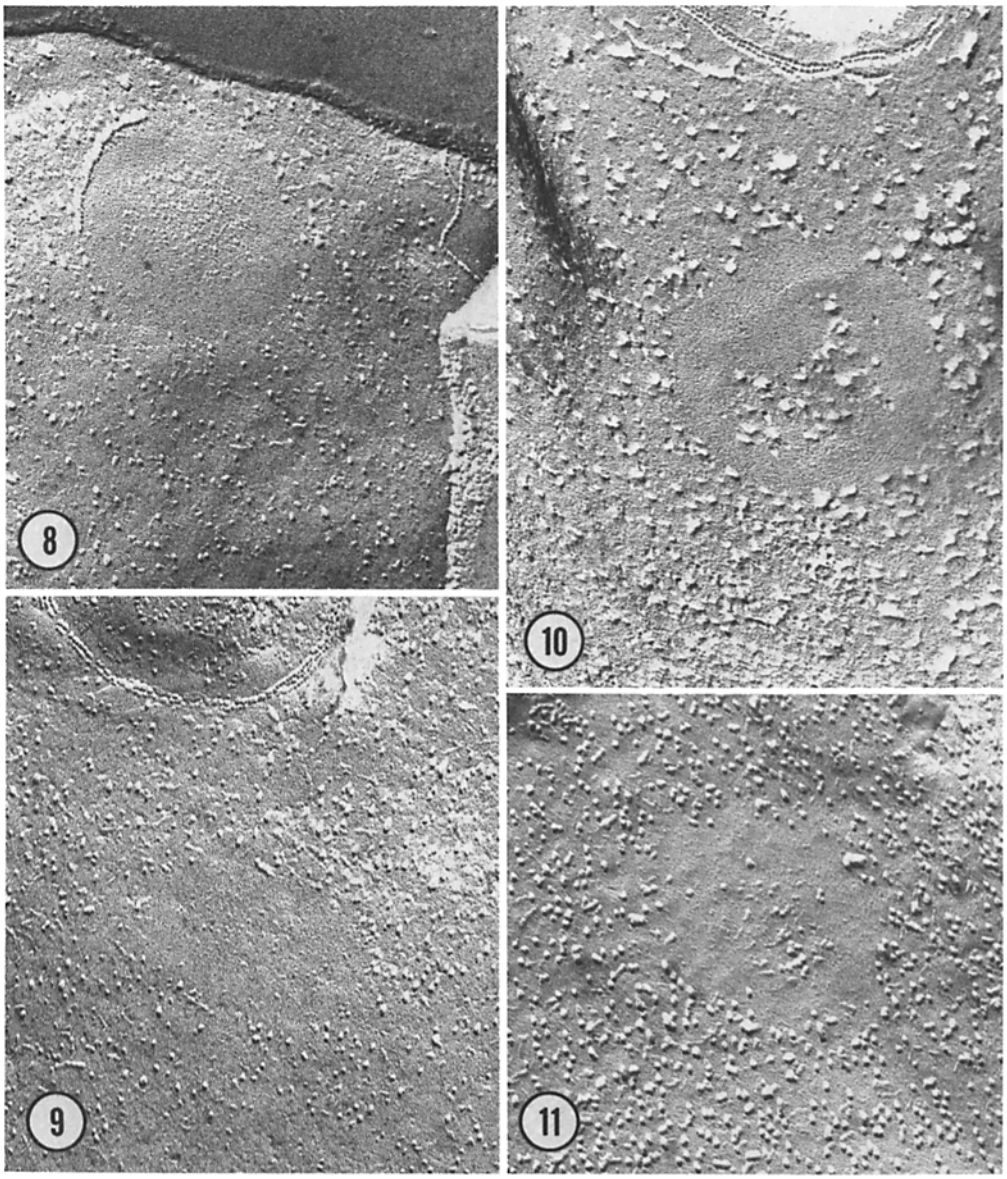

FIGURE 8 Unmated mt^- gamete (freeze-fracture, P face). An arc of particulate material defines one edge of the circular mating structure region, the center of which is seen to be finely granular. × 86,000.

FIGURE 9 Unmated mt^- gamete (freeze-fracture, P face). A small particle-free mating structure occupies the center of the field. × 86,000.

FIGURE 10 Unmated mt^- gamete (freeze-etch, P face). The center of the circular mating structure has become disrupted by the etching process (cf. Fig. 6). × 86,000.

FIGURE 11 Unmated mt^- gamete (freeze-fracture, E face). The center of the mating structure carries a cluster of particles. × 86,000.

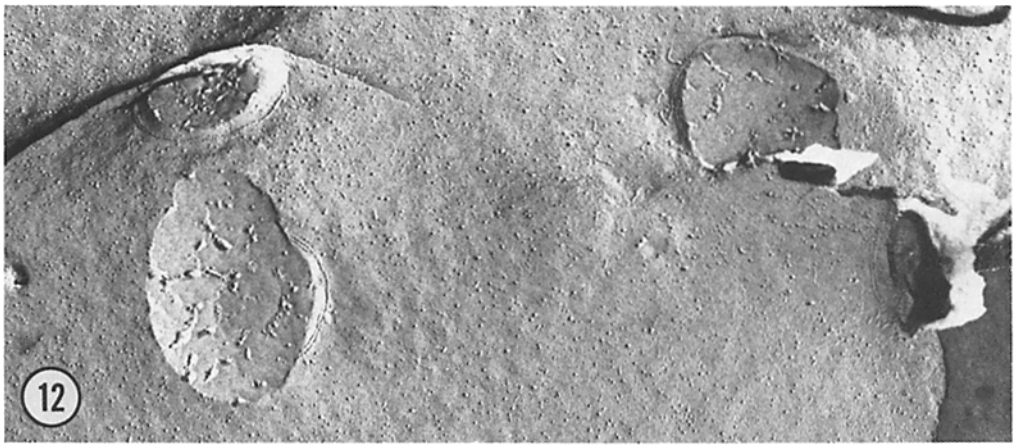

FIGURE 12 Zygote shortly after gametic cell fusion (freeze-fracture, P face), showing the four bracelet-surrounded flagella and the medial plasma membrane which has recently fused. × 43,000.

from the P face. In Fig. 13, the membrane has everted in an asymmetric fashion: the particle-bearing sector of the central region, corresponding to the *p* regions of Figs. 3 and 4, has become the tip of the projection, whereas the aparticulate sector of the central region in Fig. 4 has become the longer of the two sloping sides. In Fig. 14 the base of the fertilization tubule remains aparticulate, particles remain adherent to the tip, and a considerable expanse of additional membrane has appeared in between. This membrane is remarkable by its absence of particles. The "back side" of such a fertilization tubule—that is, the side facing away from the flagella—is shown in Fig. 15, and it too is strikingly free of intramembranous particles.

The replica shown in Fig. 16 illustrates a cell that has formed two mating structures, both of which have been stimulated to form fertilization tubules (similar "double" structures are also occasionally encountered in thin section). The fertilization tubules have both been cross-fractured proximal to the tip—the usual fate of extended tubules—and their smooth interiors are readily distinguished from the roughened interior of a flagellum. Even in such foreshortened structures (a fully extended fertilization tubule is perhaps 0.7 μm long), it is clear that considerable expanses of particle-free membrane have materialized during fertilization tubule elongation.

Figs. 17 and 18 show, respectively, end-on and side views of the fertilization tubule E face. The asymmetry of the protruding tubule is well illustrated in Fig. 17, where one of the two sides of the base is clearly longer than the other. Fig. 18 demonstrates that the E-face membrane is quite as devoid of particles as the P face (compared with Figs. 14–16).

Membrane Changes in Activated mt⁻ Mating Structures

It will be recalled from Figs. 7–10 that the unactivated *mt*⁻ mating structure is a symmetrical region with a roughened P-face center and a somewhat particulate E-face center. Activation results in the changes illustrated in Figs. 19–22. In the P face, the central region first increases its roughened texture (Fig. 19) and then takes on a sombrero topology (Fig. 20): a protuberant center, now carrying large particles, is delineated from a smooth "brim" by a somewhat depressed circular region. The corresponding differentiation in the E face is even more dramatic (Figs. 21 and 22): the central dome becomes crowded with particles, while the brim remains essentially particle free. Such images can be directly related to thin-section images (e.g., Fig. 12 of reference 18) where *mt*⁻ mating structure activation is seen to transform the dense membrane zone from a continuous layer to a peripheral rim of material surrounding membrane which lacks any dense material beneath it.

Images of Fusing Cells

Equal numbers of *mt*⁺ and *mt*⁻ gametes can be mixed at room temperature and aliquots can be fixed at 2-min intervals thereafter under conditions that dissociate agglutinating cells but preserve fused cells. In a representative experiment,


13


14


15


16

12% of the cells were found to have fused during the first 2 min, 52% had fused by 4 min, 74% by 6 min, and 100% by 10 min. Thus, less than 2 min are required for at least some cells to lose their walls (18), activate their mating structures, grow out their fertilization-tubules, and undergo fusion, meaning that the primary membrane fusion event itself must occur extremely rapidly.

Primary membrane fusion between gametes creates a cytoplasmic bridge (16, 18); this initial fusion is followed by a cytoplasmic confluence which is accompanied by a considerable amount of membrane flow and endocytosis (Fig. 1 of reference 18, and our unpublished observations). Numerous images in our replicas of mating gametes show spans of membrane connecting two cells, but it has proved impossible to determine which of these represents a primary bridge and which represents secondary zones of contact. We have therefore based our knowledge of the primary fusion process on those few replicas that could be identified with some certainty as deriving from fusing cells.

Figs. 23 and 24 show, respectively, the P and E faces of what we believe to be cytoplasmic bridges at their mt^+ "ends." The diameter of the cross-fractured bridge (350 nm) in Fig. 23 is larger than the diameter of a cross-fractured fertilization tubule (250 nm) (see, for example, Fig. 16), a change that is also apparent in thin section (16, 18). Moreover, the particle-excluding zone at the base of the bridge increases in size compared to the base of the fertilization tubule (compare Figs. 23 and 24 with Figs. 16 and 17). While these changes are of interest inasmuch as they may relate to the proposed shortening and widening of the fusion bridge during mating (16, 18), they are not directly relevant to the fusion process, since cell fusion occurs at the mt^- "end" of the cytoplasmic bridge.

The replica depicted in Fig. 25 shows what we interpret to be the E face of an mt^- gamete participating in cell fusion. The mating structure region (demarcated by arrowheads) differs from its mt^+ counterpart (Fig. 24) in that it is not asymmetric and has not undergone a broadening of the peripheral particle-free zone. On the other hand, the region is similar to an activated mt^- E face (Figs. 21 and 22) in its size, symmetry, and dense population of particules. The major difference between the activated and the fused regions is that the uninterrupted "dome" of particles in Figs 21 and 22 has been transformed in Fig. 25 into a rim of particles, well shadowed only on its under surface, which surrounds a central opening having the expected diameter (350 nm) and smooth interior of a cytoplasmic bridge (*b*). Fig. 25 is, in fact, virtually identical to images of mucocyst secretion in *Tetrahymena* (e.g., Fig. 3 of reference 43) with one very interesting exception: during secretory fusion, particles localize in the P (protoplasmic) face, whereas during gametic cell fusion the particles localize in the E (ectoplasmic) face. These localizations suggest that whatever role is played by clustered particles in membrane fusion, this role is acted out in that half of the membrane where the initial fusogenic event(s) takes place.

DISCUSSION

Differentiation of the C. reinhardtii Mating Structure

The mating structures that differentiate in *C. reinhardtii* during gametogenesis are shown in this paper to consist not only of dense cytoplasmic material (references 10, 16, 18, 48; Figs. 1 and 2) but also of specialized sectors of plasma membrane. Considerable architectural correspondence can be recognized between the cytoplasmic material and its

FIGURE 13 Activated mt^+ gamete mixed with mt^- flagella (freeze-fracture, P face) showing an early stage in fertilization tubule outgrowth, possibly corresponding to the bud stage (18). The tip of the protuberance is seen to be particulate. × 86,000.

FIGURE 14 Activated mt^+ gamete mixed with mt^- gametes at 4°C (freeze-fracture, P face). A few particles are present at the tip of the elongating fertilization tubule. × 86,000.

FIGURE 15 Activated *imp-1* mt^+ gamete mixed with mt^- gametes at room temperature (freeze-fracture, P face). The fertilization tubule is abnormally short and broad in this mutant (see Materials and Methods). × 86,000.

FIGURE 16 Activated mt^+ gamete mixed with mt^- gametes at 4°C (freeze-fracture, P face). Two fertilization tubules, both cross-fractured at proximal locations, emerge from a single cell. × 86,000.

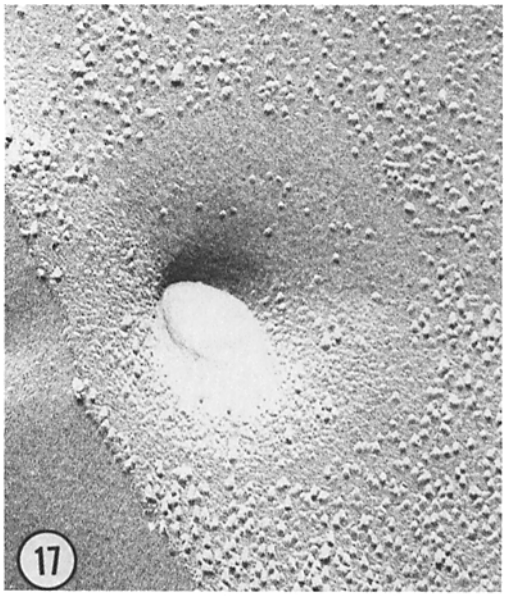

FIGURE 17 Activated mt^+ gamete mixed with mt^- flagella (freeze-fracture, E face) showing base of the fertilization tubule. × 86,000.

overlying membrane. Thus, in the unmated mt^+ cell, the "lopsided collar" configuration of the doublet zone is reflected by an asymmetric distribution of particles in the center of the membrane region (Figs. 3, 4, and 7), while in the mt^- cell the thickened region at the periphery of the dense membrane zone (Fig. 2) corresponds in position to the particle-free rim around the central particulate cluster within the membrane (Figs. 8–10). Such correspondence, in the context of the arguments presented in the previous paper (52), suggests that the dense material is capable of bringing about a unique patterning of membrane components when it associates with the membrane, an association apparently established during the mitotic cytokinesis that accompanies gametogenesis (30). It is, of course, also conceivable that the membrane differentiates first and subsequently patterns the dense material, although it then becomes difficult to speculate on the function of the dense material.

Three other instances can be cited in which a dense submembranous material effects similar kinds of changes in its overlying membrane; whether such differentiations proceed by any sort of common biochemical mechanism is not yet known. (*a*) A dense material underlies postsynaptic membranes which are found by freeze-cleave microscopy to carry particle aggregates in an otherwise particle-poor fracture face (42). (*b*) During the maturation of certain animal viruses, each dense nucleocapsid core moves to the cell surface and "clears" the overlying membrane of its usual complement of particles (5, 9). The resultant membrane then everts and envelops the viral nucleocapsid. The morphology of such budding animal viruses in thin section is often strikingly similar to that of the mt^- mating structure (e.g., compare Fig. 2 of reference 18 with Fig. 3 of reference 5), although the resemblance may well be fortuitous. (*c*) The tip of each intestinal microvillus bears a particle-free membrane region which overlies a dense submembranous material (34). This material, moreover, associates with microfilaments (33) in a manner reminiscent of the mt^+ mating structure.

While the mt^+ and mt^- mating-structure membranes exclude most of the large particles that are scattered throughout the P and E faces of the surrounding plasma membrane, they are clearly not

FIGURE 18 Activated mt^+ gamete mixed with mt^- gametes at 4°C (freeze-fracture, E face). The fertilization tubule exhibits a particle-poor membrane. Strut arrays and bracelet grooves (52) are evident around the flagellum. × 86,000.

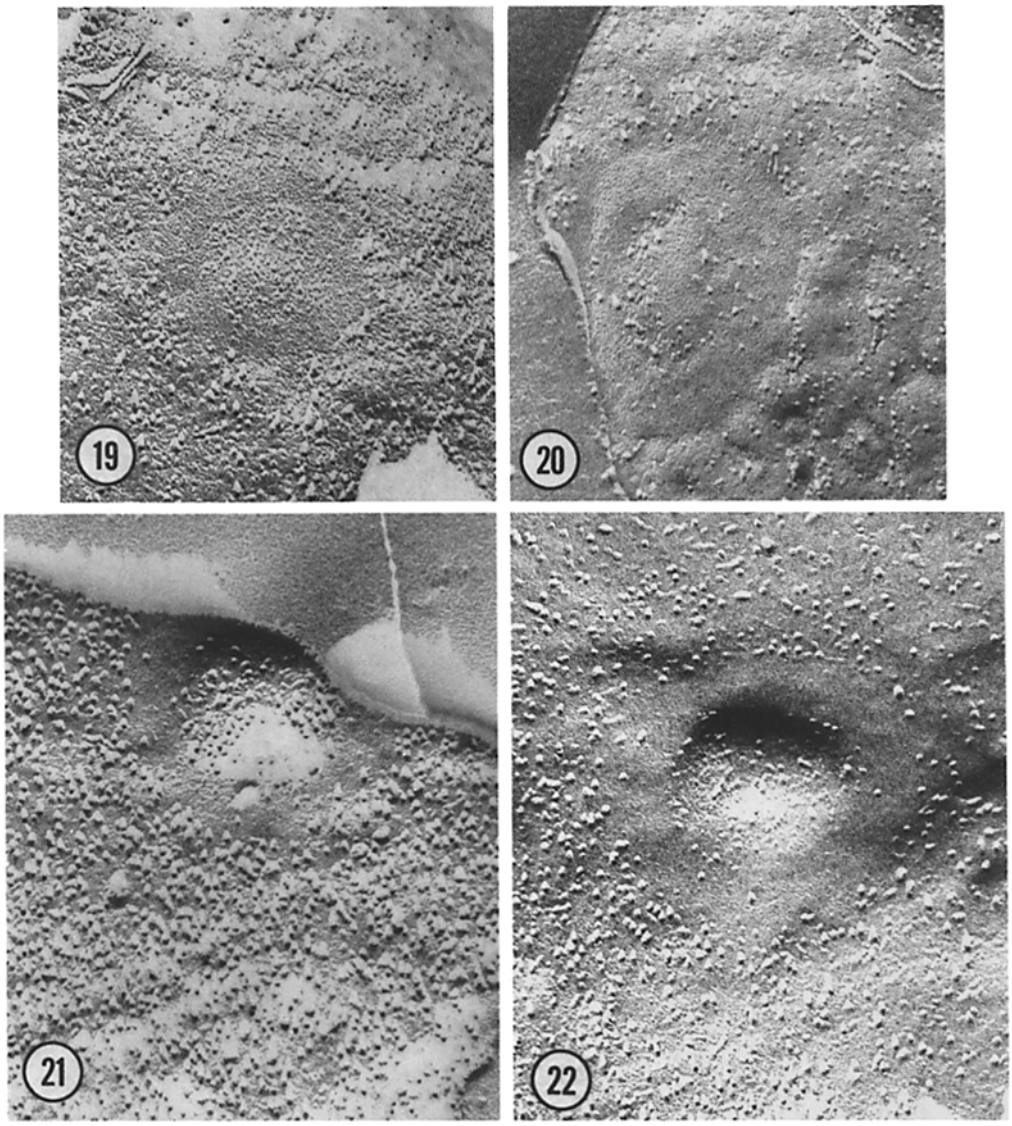

FIGURE 19 Activated mt^- gamete mixed with mt^+ flagella (freeze-fracture, P face) showing an early stage in activation, with the central particles somewhat more prominent than in the unactivated state (cf. Fig. 8). × 86,000.

FIGURE 20 Activated mt^- gamete mixed with *imp-1* gametes (freeze-fracture, P face) showing a later stage in activation, with the brim and the edge of the structure clearly demarcated by puckering. × 86,000.

FIGURES 21 and 22 Two views of activated mt^- gametes mixed with mt^+ flagella (freeze-fracture, E face) showing the prominent doming of the membrane, the concentration of particles in the central region, and the particle-free rim. × 86,000.

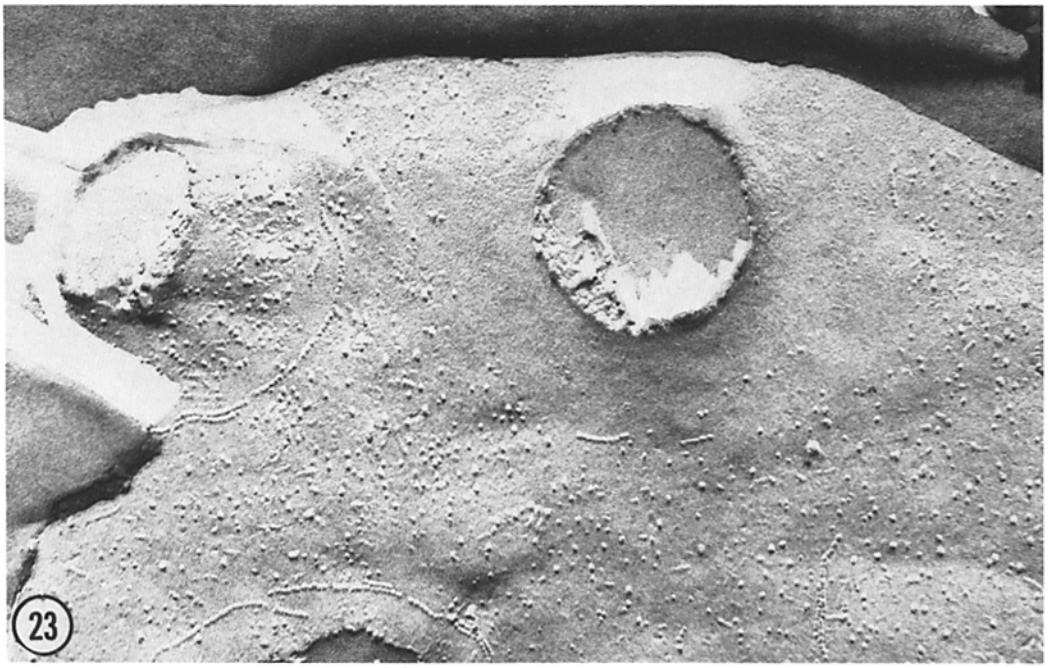
23


24

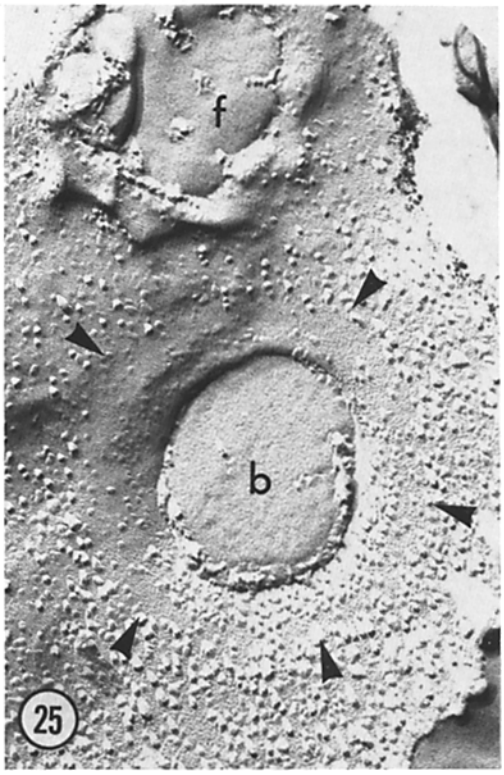
f
b
25

particle-free in the sense that artificial lipid bilayers (reviewed in reference 20) or spectrin-extracted portions of erythrocyte membranes (14) appear particle-free. The arrays of particles that are present are discussed below in relation to the role they may play in mating structure activation and/or membrane fusion.

Functional Aspects of mt⁺ Mating Structure Architecture

Our replicas indicate that the P-face cluster of large particles, denoted as region *p*, represents the sector of the *mt*⁺ membrane that will become the tip of the fertilization tubule after activation. This sector apparently lies over the "collar hole" in the doublet zone, although a corresponding "hole" is not apparent in the membrane zone material that adheres to the inner membrane leaflet (18). The less particulate sector of the *mt*⁺ central region remains with the base of the *mt*⁺ fertilization tubule and cannot thereby participate directly in cell fusion.

The entire *mt*⁺ structure region is refractory to etching compared to the surrounding plasma membrane (Fig. 6), suggesting that the region may be particularly hydrophobic (7), either intrinsically or because of its underlying dense material. Alternatively, the lipid composition and/or architecture of the mating-structure membrane may be fundamentally different from that of the surrounding membrane, which may help to explain how the particles in the surrounding lipid matrix are excluded. Lipid phase separations, for example, appear to influence particle distributions in experimentally manipulated membranes (11, 23, 45, 51).

The final feature of considerable interest regarding the *mt*⁺ mating structure is its ability to generate large expanses of particle-cleared membrane during the 1–2 min required to produce a fertilization tubule after flagellar agglutination. This feat, which can occur at 4°C (present study) and in the presence of cycloheximide (15, 32), is open to at least two kinds of interpretation. (*a*) Pre-existing plasma membrane may be transformed into fertilization-tubule membrane. To explain the accompanying loss of particles, one could assume that plasma-membrane lipid is free to flow into the fertilization tubule whereas particle-producing plasma membrane proteins are anchored in place (e.g., as envisaged for the red cell [13]) and cannot move. Alternatively, one could speculate that the combined membrane-doublet zone at the base of the growing fertilization tubule (18) acts as a sieve to exclude particles from the flowing plasma membrane. (*b*) A *de novo* assembly of new, particle-poor membrane may occur at the time of fertilization tubule outgrowth, perhaps in coupling with microfilament assembly. The rapidity of tubule outgrowth would seem to require that such membrane precursors be produced and stored by the *mt*⁺ gamete in anticipation of mating.

Several kinds of experimental manipulations cause membranes to lose their component intramembranous particles and to "blister out"; these include treatment of lymphocytes with dimethyl sulfoxide (31) and removal of spectrin from erythrocyte membranes (14). The particle-cleared membrane which overlies maturing flu virus (5) also readily buds from the adjacent plasma membrane. It therefore seems reasonable to postulate that, regardless of its mode of origin, the particle-

FIGURE 23 Presumed *mt*⁺ end of cytoplasmic bridge (freeze-fracture, P face) in a mixed suspension of gametes allowed to interact for 10 min before freezing. The broad particle-free base and the absence of particles at the point of cross-fracture identify this as the *mt*⁺ end of bridge. Two flagellar bracelets are also present in the field. × 86,000.

FIGURE 24 Presumed *mt*⁺ end of cytoplasmic bridge (freeze-fracture, E face) in a mixed suspension of gametes allowed to warm to room temperature after agglutination in the cold. The similarity of this replica to Fig. 17 indicates that the *mt*⁺ end of the bridge is represented. The narrow midfield fold extends well out into the plasma membrane and is presumably an artifact. × 86,000.

FIGURE 25 Presumed *mt*⁻ end of cytoplasmic bridge (freeze-fracture, E face) shortly after fusion. The center of the bridge (*b*) is surrounded by a dense grouping of particles which are well shadowed beneath and to the right of the central opening and poorly shadowed above it. This particle-rich ring is in turn surrounded by a particle-free rim. Arrowheads mark the outer boundary of the particle-free rim. Flagellum at *f*. × 86,000.

cleared membrane of the fertilization tubule would be readily "pushed out" by the underlying microfilament system.

Functional Aspects of mt⁻ Mating Structure Architecture

The *mt*⁻ mating-structure membrane also excludes membrane particles, perhaps under the aegis of its associated brim of dense cytoplasmic material (Fig. 2, arrows), but its architecture is otherwise fundamentally different from that of *mt*⁺. The central mass of particulate material is readily etched (Fig. 10), suggesting a relatively hydrophilic make-up, either intrinsically or because the underlying dense material does not provide the postulated hydrophobicity of the *mt*⁺ material. Mating-structure activation, moreover, causes a doming of the central region and brings about an apparent increase in both the number and the size of the particles in this region, most dramatically in the E face. While an alteration in particle size or number is usually interpreted as a migration of particles into a region (12, 24, 35) in concert with the fluid-mosaic model (47), we see no particles "in transit" in the exclusion zone that surrounds the central cluster. We therefore favor what can be termed a selective insertion model. We propose that protein molecules are sequestered within the center of the cytoplasmic membrane zone and barely protrude into the overlying lipid bilayer until activation occurs. Activation releases this constraint and the proteins, perhaps modified chemically or in conformation, move into the membrane interior, localizing in the outer E face of the mating structure where they appear as large, abundant particles.

The Fusion Process

When the tip of the fertilization tubule meets the activated *mt*⁻ zone, fusion appears to occur within the particle-rich sector of the *mt*⁻ membrane (the expected site of fusion in the model of Poste and Alison [41]) and not at the particle-cleared periphery (the expected site of fusion in the model of Ahkong et al. [3]). We therefore conclude that these *mt*⁻ particles play an active role in the fusion process, and note with interest that the temperature-sensitive *gam-1* mutation of *C. reinhardtii*, which prevents fusion at restrictive temperatures, is expressed only in *mt*⁻ cells (15).

Beyond this, the mechanism of fusion remains unknown, and we can only offer our own speculative models. One possibility is that the few particles at the tip of the fertilization tubule and/or the overlying fuzzy material (Fig. 1) make specific contacts with the *mt*⁻ particle dome to produce or stimulate the "destabilization" conditions (29) required for bilayer fusion. The studies of van der Bosch and McConnell (49), which suggest that protein-to-protein interactions induce lipid phase separations (21, 22, 46) followed by membrane fusion, are of direct interest in this regard, as is the demonstration by Scheid and Choppin (44) of a direct participation in cell fusion by a specific surface glycoprotein of Sendai virions. Other possibilities are that the fertilization tubule tip contains a specific class of lipid, that the *mt*⁻ particle dome possesses a lipase activity for that lipid, and that the *mt*⁺/*mt*⁻ specificity of fusion, plus the fusion event itself, results from such an enzyme-substrate interaction (see, in this regard, references 26 and 40). Such models are, fortunately, amenable to experimental test, and we are presently initiating an extensive study on the effects of temperature, ionic conditions, and gene mutation on the gametic fusion process.

Received for publication 2 June 1976, and in revised form 17 September 1976.

REFERENCES

1. AHKONG, Q. F., F. C. CRAMP, D. FISHER, J. I. HOWELL, W. TAMPION, M. VERRINDER, and J. A. LUCY. 1973. Chemically-induced and thermally-induced cell fusion: lipid-lipid interactions. *Nature (Lond.)*. **242:**215–217.
2. AHKONG, Q. F., D. FISHER, W. TAMPION, and J. A. LUCY, 1973. The fusion of erthrocytes by fatty acids, esters, retinol and α-tocopherol. *Biochem. J.* **136:**147–155.
3. AHKONG, Q. F., D. FISHER, W. TAMPION, and J. A. LUCY. 1975. Mechanisms of cell fusion. *Nature (Lond.)* **253:**194–195.
4. AHKONG, A. F., W. TAMPION, and J. A. LUCY. 1975. Promotion of cell fusion by divalent cation ionophores. *Nature (Lond.)*. **256:**208–209.
5. BÄCHI, T., W. GERHARD, J. LINDENMANN, and K. MÜHLETHALER. 1969. Morphogenesis of influenza A virus in Ehrlich ascites tumor cells as revealed by thin-sectioning and freeze-etching. *J. Virol.* **4:**769–776.
6. BERGMAN, K., U. W., GOODENOUGH, D. A. GOODENOUGH, J. JAWITZ, and H. MARTIN. 1976. Gametic differentiation in *Chlamydomonas reinhardtii*. II. Flagellar membranes and the agglutination reaction. *J. Cell Biol.* **67:**606–622.

7. BRANTON, D. 1966. Fracture faces of frozen membranes. *Proc. Natl. Acad. Sci. U. S. A.* **55**:1048–1056.
8. BREISBLATT, W., and S. OHKI. 1975. Fusion in phospholipid spherical membranes. I. Effect of temperature and lysolecithin. *J. Membr. Biol.* **23**:385–401.
9. BROWN, D. T., M. R. F. WAITE, and E. R. PFEFFERKORN. 1972. Morphology and morphogenesis of Sindbis virus as seen with freeze-etching techniques. *J. Virol.* **10**:524–536.
10. CAVALIER-SMITH, T. 1975. Electron and light microscopy of gametogenesis and gamete fusion in *Chlamydomonas reinhardtii*. *Protoplasma.* **86**:1–18.
11. CHEN, Y. S., and W. L. HUBBELL. 1973. Temperature- and light-dependent structural changes in rhodopsin-lipid membranes. *Exp. Eye Res.* **17**:517–532.
12. DECKER, R. S., and D. S. FRIEND. 1974. Assembly of gap junctions during amphibian neurulation. *J. Cell Biol.* **62**:32–47.
13. ELGSAETER, A., and D. BRANTON. 1974. Intramembrane particle aggregation in erythrocyte ghosts. I. The effects of protein removal. *J. Cell Biol.* **63**:1018–1030.
14. ELGSAETER, A., D. M. SHOTTON, and D. BRANTON. 1976. Intramembrane particle aggregation in erythrocyte ghosts. II. The influence of spectrin aggregation. *Biochim. Biophys. Acta.* **426**:101–122.
15. FOREST, C. L., and R. K. TOGASAKI, 1975. Selection for conditional gametogenesis in *Chlamydomonas reinhardi*. *Proc. Natl. Acad. Sci. U. S. A.* **72**:3652–3655.
16. FRIEDMANN, I., A. L. COLWIN, and L. H. COLWIN. 1968. Fine-structural aspects of fertilization in *Chlamydomonas reinhardi*. *J. Cell Sci.* **3**:115–128.
17. GOODENOUGH, U. W., C. HWANG, and H. MARTIN. 1976. Isolation and genetic analysis of mutant strains of *Chlamydomonas reinhardi* defective in gametic differentiation. *Genetics.* **82**:169–186.
18. GOODENOUGH, U. W., and R. L. WEISS. 1975. Gametic differentiation in *Chlamydomonas reinhardtii*. III. Cell wall lysis and microfilament-associated mating structure activation in wild-type and mutant strains. *J. Cell Biol.* **67**:623–637.
19. GRATZL, M., and G. DAHL. 1976. Ca^{++}-induced fusion of Golgi-derived secretory vesicles isolated from rat liver. *FEBS (Fed. Eur. Biochem. Soc.) Lett.* **62**:142–153.
20. GULIK-KRZYWICKI, T. 1975. Structural studies of the associations between biological membrane components. *Biochim. Biophys. Acta.* **415**:1–28.
21. ITO, T., S. OHNISHI, M. ISHINAGA, and M. KITO. 1975. Synthesis of a new phosphatidylserine spin-label and calcium-induced lateral phase separations in phosphatidylserine-phosphatidylcholine membranes. *Biochemistry.* **14**:3064–3069.
22. JACOBSON, K., and D. PAPAHADJOPOULOS. 1975. Phase transitions and phase separations in phospholipid membranes induced by changes in temperature, pH, and concentration of bivalent cations. *Biochemistry.* **14**:152–161.
23. JAMES, R., D. BRANTON, B. WISNIESKI, and A. KEITH. 1972. Composition, structure and phase transition in yeast fatty acid auxotroph membranes: spin labels and freeze-fracture. *J. Supramol. Struct.* **1**:38–49.
24. JOHNSON, R., M. HAMMER, J. SHERIDAN, J. P. REVEL. 1974. Gap junction formation between reaggregated Novikoff hepatoma cells. *Proc. Natl. Acad. Sci. U. S. A.* **71**:4536–4540.
25. KANTOR, H. L., and J. H. PRESTEGARD. 1975. Fusion of fatty acid containing lecithin vesicles. *Biochemistry.* **14**:1790–1794.
26. KORN, E. D., B. BOWERS, S. BATZRI, S. R. SIMMONS, and E. J. VICTORIA. 1974. Endocytosis and exocytosis: role of microfilaments and involvement of phospholipids in membrane fusion. *J. Supramol. Struct.* **2**:517–528.
27. KOSOWER, N. S., E. M. KOSOWER, and P. WEGMAN. 1975. Membrane mobility agents. II. Active promoters of cell fusion. *Biochim. Biophys. Acta* **401**:530–534.
28. LENEVEU, D. M., R. P. RAND, and V. A. PARSEGIAN. 1976. Measurement of forces between lecithin bilayers. *Nature (Lond.).* **259**:601–603.
29. LUCY, J. A. 1975. Aspects of the fusion of cells *in vitro* without viruses. *J. Reprod. Fertil.* **44**:193–205.
30. MARTIN, N. C., and U. W. GOODENOUGH. 1975. Gametic differentiation in *Chlamydomonas reinhardtii*. I. Production of gametes and their fine structure. *J. Cell Biol.* **67**:587–605.
31. MCINTYRE, J. A., N. B. GILULA, and M. J. KARNOVSKY. 1974. Cryoprotectant-induced redistribution of intramembranous particles in mouse lymphocytes. *J. Cell Biol.* **60**:192–203.
32. MINAMI, S. 1976. Protein synthesis during differentiation of *Chlamydomonas reinhardi*. Ph.D. thesis, Harvard University, Cambridge, Mass.
33. MOOSEKER, M. S., and L. G. TILNEY. 1975. Organization of an actin filament-membrane complex. Filament polarity and membrane attachment in the microvilli of intestinal epithelial cells. *J. Cell Biol.* **67**:725–743.
34. MOOSEKER, M. S., and L. G. TILNEY. 1975. Actin filament-membrane attachment: are membrane particles involved? *J. Cell Biol.* **67**(2, Pt.2):293a (Abstr.).
35. OJAKIAN, G. K., and P. SATIR. 1974. Particle movements in chloroplast membranes: quantitative measurements of membrane fluidity by the freeze-fracture technique. *Proc. Natl. Acad. Sci. U. S. A.* **71**:2052–2056.
36. OKADA, Y., J. KIM, Y. MAEDA, and I. KOSEKI. 1974. Specific movement of cell membranes fused

with HVJ (Sendai virus). *Proc. Natl. Acad. Sci. U. S. A.* **71**:2043–2047.

37. PAPAHADJOPOULOS, D., G. POSTE, and B. E. SCHAEFFER. 1973. Fusion of mammalian cells by unilamellar lipid vesicles: influence of lipid surface charge, fluidity and cholesterol. *Biochim. Biophys. Acta.* **323**:23–42.
38. PAPAHADJOPOULOS, D., G. POSTE, B. E. SCHAEFFER, and W. J. VAIL. 1974. Membrane fusion and molecular segregation in phospholipid vesicles. *Biochim. Biophys. Acta* **352**:10–28.
39. PERETZ, H., Z. TOISTER, Y. LASTER, and A. LOYTER. 1974. Fusion of intact human erythrocytes and erythrocyte ghosts. *J. Cell Biol.* **63**:1–11.
40. POOLE, A. R., J. I. HOWELL, and J. A. LUCY. 1970. Lysolecithin and cell fusion. *Nature (Lond.).* **227**:810–814.
41. POSTE, G., and A. C. ALISON. 1973. Membrane fusion. *Biochim. Biophys. Acta.* **300**:421–465.
42. SANDRI, C., K. AKERT, R. B. LIVINGSTON, and H. MOOR. 1972. Particle aggregations at specialized sites in freeze-etched postsynaptic membranes. *Brain Res.* **41**:1–16.
43. SATIR, B. 1974. Ultrastructural aspects of membrane fusion. *J. Supramol. Struct.* **2**:529–537.
44. SCHEID, A., and P. W. CHOPPIN. 1974. Identification of biological activities of paramyxovirus glycoproteins. Activation of cell fusion, hemolysis, and infectivity by proteolytic cleavage of an inactive precursor protein of Sendai virus. *Virology.* **57**:475–490.
45. SHECHTER, E., L. LETELLIER, and T. GULIK-KRZYWICKI. 1974. Relations between structure and function in cytoplasmic membrane vesicles isolated from an *Escherichia coli* fatty-acid auxotroph. High-angle X-ray diffraction, freeze-etch electron microscopy, and transport studies. *Eur. J. Biochem.* **49**:61–76.
46. SHIMSHICK, E. J., and H. M. MCCONNELL. 1973. Lateral phase separations in phospholipid membranes. *Biochemistry.* **12**:2351–2360.
47. SINGER, S. J., and G. L. NICOLSON. 1972. The fluid mosaic model of the structure of cell membranes. *Science (Wash. D.C.).* **175**:720–731.
48. TRIEMER, R. E., and R. M. BROWN. 1975. Fertilization in *Chlamydomonas reinhardi,* with special reference to the structure, development, and fate of the choanoid body. *Protoplasma.* **85**:99–107.
49. VAN DER BOSCH, J., and H. M. MCCONNELL. 1975. Fusion of dipalmitoyl-phosphatidylcholine vesicle membranes induced by Concanavalin A. *Proc. Natl. Acad. Sci. U. S. A.* **72**:4409–4413.
50. VAN DER BOSCH, J., C. SCHUDT, and D. PETTE. 1973. Influence of temperature, cholesterol, dipalmitoylecithin and Ca^{++} on the rate of muscle cell fusion. *Exp. Cell Res.* **82**:433–438.
51. VERKLEIJ, A. J., P. H. J. VERVERGAERT, L. L. M. VAN DEENEN, and P. F. ELBERS. 1972. Phase transitions of phospholipid bilayers and membranes of *Acholeplasma laidlawii* B visualized by freeze fracturing electron microscopy. *Biochim. Biophys. Acta.* **288**:326–332.
52. WEISS, R. L., D. A. GOODENOUGH, and U. W. GOODENOUGH. 1977. Membrane particle arrays associated with the basal body and with contractile-vacuole secretion in *Chlamydomonas. J. Cell Biol.* **72**:133–143.